A Combined Experimental and Quantum Chemical Study on the Putative Protonophoric Activity of Thiocyanate

Peter Schönfeld,* Luis Montero,† and Jürgen Fabian‡

*Institut für Biochemie, Otto-von-Guericke-Universität Magdeburg, D-39120 Magdeburg, Germany; †Laboratorio de Química Computacional y Teórica, Facultad de Química, Universidad de La Habana, Havana 10400, Cuba; and ‡Institut für Organische Chemie, Technische Universität Dresden, D-01062 Dresden, Germany

ABSTRACT Inhibition of gastric acid secretion by thiocyanate is explained by a protonophoric mechanism assuming that thiocyanate induces a H^+ back flux from the acidic gastric lumen into the parietal cells of gastric mucosa. Protonophoric activity of thiocyanate was examined by swelling measurements using rat liver mitochondria and theoretically by quantum chemical methods. Mitochondria suspended in K-thiocyanate medium plus nigericin (an H/K-exchanger) swelled when the medium pH was acidic, indicating that SCN^- initiates a transfer of H^+ across the inner membrane. To rationalize the protonophoric activity of thiocyanate, we considered the dehydration of SCN^- to be critical for transmembranal H^+ transfer. For modeling this process, various hydrate clusters of SCN^- and Cl^- were generated and optimized by density functional theory (DFT) at the B3-LYP/6-311++G(d,p) level. The cluster hydration energy was lower for SCN^- than for Cl^-. The total Gibbs free energies of hydration of the ions were estimated by a hybrid supermolecule-continuum approach based on DFT. The calculated hydration energies also led to the conclusion that SCN^- is less efficiently solvated than Cl^-. Due to the easier removal of the hydration shell of SCN^- relative to Cl^-, SCN^- is favored in going across the membrane, giving rise to the protonophoric activity.

INTRODUCTION

The parietal cells of the gastric mucosa secrete a solution of hydrogen chloride in the glandular lumen after stimulation by histamine, acetylcholine, and gastrin (1). This process consists of several steps: i), generation of H^+ and HCO_3^- from water and carbon dioxide by the carbonic anhydrase inside of parietal cells, ii), H^+ ejection from cytosol to gastric lumen by an ATP-driven K^+/H^+-antiporter embedded in the apical membrane, iii), release of Cl^- ions from cytosol to glandular lumen by a Cl^- anion channel also embedded in the apical membrane, and iv), import of plasma Cl^- anions by counterexchange across the basolateral membrane for HCO_3^- delivered by the carbonic anhydrase reaction.

Thiocyanate is also long known as a potent inhibitor of gastric acid secretion (2). For explanation, it has been proposed that thiocyanate induces a backflux of H^+ from the acidic lumen into parietal cells of gastric mucosa, thereby decreasing the net secretion of hydrogen chloride (3–6). A simple protonophoric mechanism of thiocyanate-mediated transmembranal H^+ back flux is shown in Fig. 1. At the interface between the mucosal membrane and acidic gastric lumen, unprotonated thiocyanate traps H^+. Protonated thiocyanate permeates the membrane and releases an H^+ into the cytosol of parietal cells at the opposite membrane. Finally, the thiocyanate anion returns more or less dehydrated by permeating a Cl^- channel to the membrane-lumen interface where it again traps H^+. Proposed protonophoric activity of thiocyanate does not contrast with acidic power of thiocyanic acid ($pK_a = -1.28$ (7)). At a luminal pH < 4, the concentration of protonated thiocyanate within the aqueous glandular lumen was estimated to be sufficient for H^+ backflux to proceed at a rate equal to the rate of HCl secretion (8).

In general, SCN^- is transported by Cl^- channels across biological membranes. Even though SCN^- and Cl^- have similar physicochemical properties, in most Cl^- channels, SCN^- shows a higher permeability than Cl^- itself (9). In addition, it has been demonstrated that thiocyanate permeates black lipid ''membranes'' as anion and much faster in the protonated form. The latter suggests that protonated thiocyanate permeates biological membranes by passing protein-free hydrophobic regions (3).

Permeation of monovalent anions through bilayer membranes has been attributed to a ''solubility-diffusion'' mechanism (10,11). According to this view, an anion enters the hydrophobic phase after splitting from its hydrate shell and, afterwards, permeates across the bilayer membrane. A permeation of chloride and thiocyanate as bare ions suggests that the dehydration of hydrated anions is the critical step for the overall transmembranal H^+ backflux. To date, less is known about the hydration of thiocyanate.

In the absence of experimental data, hydration energies were estimated theoretically. Although Monte Carlo (MC) and molecular dynamics (MD) simulations are able, in principle, to predict relative hydration energies (12,13), comparable data about SCN^- and Cl^- are missing.

Former MC and MD calculations, however, provided useful information about microhydrated structures of ions in aqueous solution. Thus, MD calculation of the water-SCN^- system indicated a pronounced first and partially ordered second hydration shell (14). According to neutron diffraction

Submitted January 4, 2005, and accepted for publication June 2, 2005.

Address reprint requests to Peter Schönfeld, Tel.: 49-391-67-15892; Fax: 49-391-67-15898; E-mail: peter.schoenfeld@medizin.uni-magdeburg.de.

0006-3495/05/09/1504/12 $2.00

doi: 10.1529/biophysj.105.059006

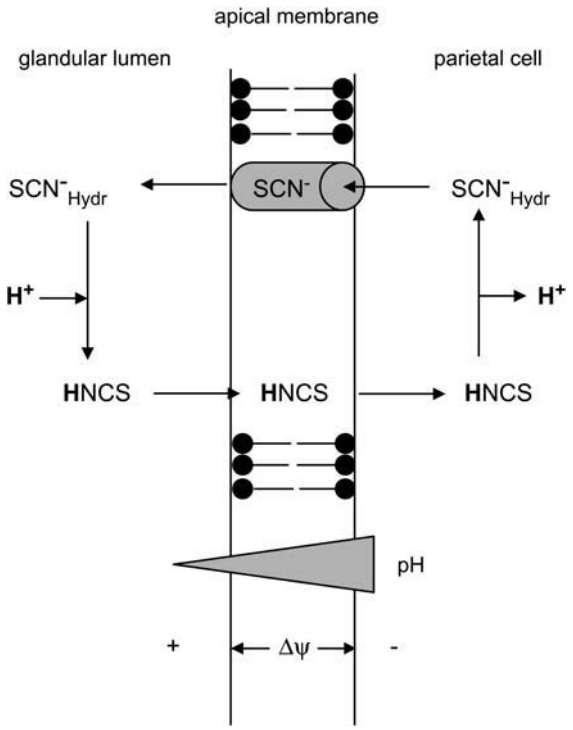

FIGURE 1 Putative mechanism of thiocyanate-mediated transmembranal H^+ transfer in parietal membranes. The thiocyanate anion (SCN^-_{Hydr}) reacts with H^+ to give isothiocyanic acid (HNCS) at the luminal side of the apical membrane. HSCN crosses the hydrophobic phase of the membrane rapidly in the dehydrated form (3) and dissociates at the cytosolic side into H^+ and SCN^-. Liberated SCN^- permeates back into the luminal side by the assistance of a Cl^- channel (5). The driving force of the cycling process is the electrochemical gradient, with ΔpH as main component at the apical membrane of the parietal cell. This gradient is generated by the ATP-dependent H^+/K^+ antiporter (not shown). Extrusion of SCN^- is supported by its concentration gradient (cytosol → lumen) and the membrane potential ($\Delta\psi$; inside negative). In summary, ΔpH-supported cycling of thiocyanate ($HSCN/SCN^-$) across the apical membrane of parietal cells reduces net secretion of hydrogen chloride into the glandular lumen.

measurements (15), there are 1.8 ± 0.2 water molecules coordinated to SCN^- with an intermolecular $N^{\cdot\cdot}H$ distance of ~2.16 Å. Hydrogen bonds are obviously formed between water and the solute molecule. The neutron diffraction study of Mason et al. (16) resulted in ~1 hydrogen bonded water molecule and ~2 water molecules weakly interacting through ''hydration bonds''. The formation of the hydrates $Cl^-(H_2O)_N$ was studied by MD (17,18), MC (19), and quantum chemistry/molecular mechanics (QM/MM) (20). The theoretical studies resulted in super molecular structures with coordination numbers N between 5 and 6. The hydration number of 6 was derived experimentally by an infrared study (21). According to Degrève et al. (19), chloride surrounded by the first hydration shell is immersed in a medium exactly like the bulk water.

As detailed below, first-principles methods opened the way to calculate hydration number and cluster hydration energies. However, the energy of hydration is not only determined by the energy of the microscopic water-anion cluster but also by the electrostatic interaction between the hydrate complex and the solvent's dielectric surroundings. The effect of bulk water is calculated by placing the supermolecular hydrate in a cavity surrounded by the dielectric continuum. Hybrid supermolecule-continuum models proved to be useful to calculate total hydration energies (e.g., Tuñón et al. (22)) and were applied to halide anions (23,24). Along these lines the solute is treated quantum mechanically, and the remaining bulk solvent is approximated by a dielectric continuum model.

In this study, we examined proposed protonophoric activity of thiocyanate by application nonrespiring rat liver mitochondria. These cell organelles respond with great sensitivity to net uptake of solutes. Mitochondria are surrounded by two membrane systems, an outer membrane free diffusible by solutes (up to a molecular mass of 5 kd) and a folded inner membrane creating an effective barrier for the permeation of solutes. As a consequence of the folded inner membrane, net solute uptake increases the mitochondrial matrix volume, which can be quantified easily by swelling measurements. Then, we analyzed the energetic changes connected with the protonophoric mechanism of thiocyanate by quantum chemical methods. Data calculated for the thiocyanate-mediated H^+ transfer were compared with those for the chloride-mediated H^+ transfer.

EXPERIMENTAL METHODS

Liver mitochondria were prepared from adult female Wistar rats (average weight 150–180 g) by differential centrifugation according to our standard protocol. The final pellet was resuspended in 0.25 M sucrose (25–35 mg of mitochondrial protein per mL). The protein content in the mitochondrial stock suspension was determined by the biuret method. Movement of SCN^- or Cl^- anions as well as their protonated forms across the inner mitochondrial membrane was examined by applying the swelling assay (25). Briefly, mitochondria (1 mg of mitochondrial protein per mL) were suspended in medium composed of 120 mM K-thiocyanate or 120 mM K-chloride plus 10 mM Tris, 0.5 mM EDTA, and 1 μM of the respiratory-chain inhibitor antimycin A and were supplemented either with valinomycin or nigericin. Suspensions of mitochondria scatter light due to the difference in the refractive index between matrix content and surrounding medium. For illustration, net uptake of KSCN plus water in mitochondria driven by osmotic support (SCN^- goes by itself and that of K^+ is valinomycin mediated) increases the matrix volume (swelling). Consequently, the difference in the refractive index between matrix and medium decreases, which is measured photometrically as decrease in the light scattering. Swelling was recorded at 540 nm using a Varian Cary 3E spectrophotometer equipped with a thermostated (25°C) and magnetically stirred sampling unit.

COMPUTATIONAL METHODS

The water-anion cluster hydration energy (also known as binding or interaction energy of hydration) is defined as the difference in energy between the microsolvated anion and the bare anion and free water. The cluster hydration energy is negative for exothermic reactions. For the first hydration shell, the gain in energy is mainly determined by the H-bonds between the anion and the surrounding nearest-neighbor water molecules,

but H-bonds between water molecules contribute, to some extent, to the cluster hydration energy.

Cluster hydration energies of anions were mainly calculated by ab initio methods of quantum chemistry in the past. Thus, extensive studies on hydrated Cl^- were performed by MØller-Plesset second-order perturbation theory (17,26). In studying the effects of microsolvation, the density functional theory (DFT) is a useful alternative approach (23). Hydrates in this study were exclusively calculated by Kohn-Sham DFT using the B3-LYP functional (27). The calculations were performed with the Pople-type valence triple-ζ basis set with two sets of diffuse functions and two sets of polarization functions (6-311++G(d,p) basis set). To treat supermolecular H-bond structures, this extended basis set imparts the calculation for the necessary flexibility (27,28). To reduce the basis set superposition error (BSSE) (29,30), the energies were also calculated by the more extended Pople-type basis set 311++G(3df,3pd) using the B3-LYP/6-311++G(d,p) optimized geometries. Structures are only presented and discussed if all $3N - 6$ frequencies were positive, where N is the number of atoms. The gas phase normal mode vibrational frequencies were calculated within the harmonic approximation. These frequencies entered the calculations of gas phase enthalpies and entropies and, finally, of Gibbs free energies.

To estimate the bulk solvent effects in water, different methods found practical applications (see, e.g., Satchell and Smith (31)). The polarizable continuum model (PCM) variation of the self-consistent reaction field method (32) was employed in this study. The PCM method is comparable in its performance to the Langevin dipole method (33). The PCM method has been recently reviewed by Cammi et al. (34) and Tomasi (35). To calculate approximate Gibbs free energies of hydration, the DFT optimized ion-water clusters were embedded in the dielectric continuum of water with the dielectric constant $\varepsilon = 78.39$. The PCM calculations were performed at the same DFT level used for the calculation of the supermolecular hydrate structures. All calculations were carried out by the Gaussian98 suite of programs (36). The PCM method used was the option implemented by Barone et al. (37) in the Gaussian program.

RESULTS AND DISCUSSION

Swelling measurements

Rat liver mitochondria in K-thiocyanate medium swell only slowly due to a poor permeability of the inner membrane to K^+ (Fig. 2 *A*). Addition of valinomycin (a K-ionophore) induces rapid swelling, resulting from the simultaneous uptake of K^+ and of SCN^- (indicated as decrease in light scattering, *trace a*). In contrast, when nigericin (a K/H-

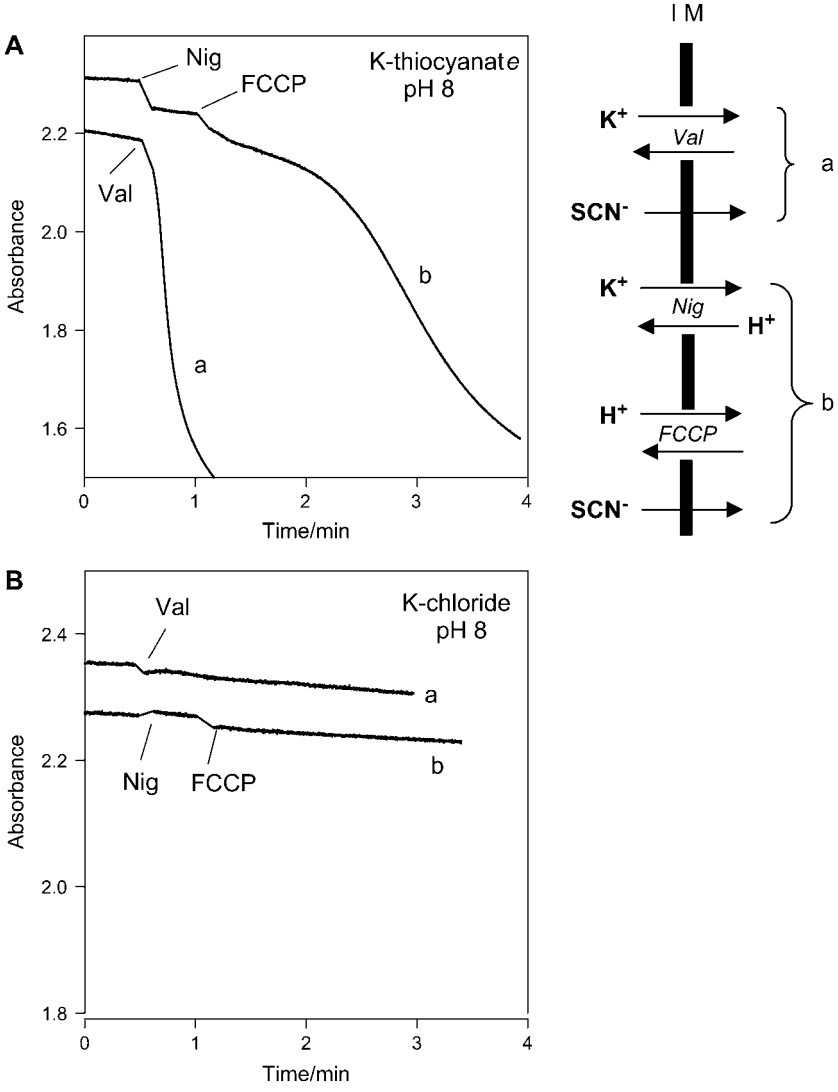

FIGURE 2 Effect of valinomycin or nigericin on the permeability of the inner mitochondrial membrane to thiocyanate and chloride anion. Mitochondria (1 mg of protein/mL) were suspended in K-thiocyanate or K-chloride medium (pH 8.0). Valinomycin (Val) and nigericin (Nig) were added to a concentration of 0.5 and 1 μM. FCCP (carbonyl cyanide p-trifluoromethoxyhydrazone) was 0.1 μM. Permeability of the inner mitochondrial membrane to ions is reflected by the decrease in light absorbance. The scheme to the right shows the ionophore-mediated transport of K^+ (Val, Nig) and of H^+ (FCCP, Nig) from the medium across the inner mitochondrial membrane (IM) into the matrix compartment. These ionophores permeate from left to right as K^+-Val, K^+-Nig^-, and FCCPH but return from right to left as Val, $FCCP^-$, and NigH. Consequently, permeation of K^+ and H^+ is due to catalytic operation of the ionophores.

exchanger) was added, swelling was not stimulated (*trace b*). Under this condition the permeation of SCN^- cannot be paralleled by a net cation uptake in mitochondria. But, mitochondria started to swell in the presence of nigericin if the protonophore FCCP was added. FCCP enables SCN^- permeation to be joined by net proton uptake. No swelling was seen when mitochondria were in K-chloride medium either supplemented with valinomycin or nigericin plus FCCP (Fig. 2 *B*).

In principle, SCN^- and Cl^- can rapidly enter mitochondria across the inner membrane anion channel (IMAC) (38); however, this channel should be closed under the applied incubation conditions. An activation of IMAC demands depletion of mitochondria from matrix-bound Mg^{2+}. In addition, it is known that fatty acids can operate as protonophores and that special proteins of the inner membrane, such as the ADP/ATP carrier, accelerate the permeation of fatty acid anions (for a review, see Wojtczak and Schönfeld (39)). Both the smallness of SCN^- and charge delocalization make it unlike that membrane proteins contribute essentially to SNC^- permeation. In summary, different rates of swelling in valinomycin-containing media reflect the permeability of the hydrophobic core of the inner membrane to SCN^- and Cl^-.

Protonophoric activity of SCN^- was examined by recording swelling in media adjusted to pH values ranging from slightly alkaline to acidic. Fig. 3 shows that a change in the medium pH does not affect swelling. However, when the K-thiocyanate medium was acidic, an addition of nigericin initiates swelling in a pH-dependent manner (Fig. 3 *A*). This observation clearly indicates that SCN^- is able to mediate the H^+ transfer across the inner membrane, similar to FCCP (Fig. 2 *A*, *trace b*) but with much lesser potency. In contrast, acidification of K-chloride medium does not stimulate swelling after addition of nigericin (Fig. 3 *B*).

On the first view, it looks strange that thiocyanate as a low-affinity proton acceptor becomes protonated at slightly acidic pH to a sufficient extent to induce a measurable transmembranal H^+ transfer in mitochondria. Furthermore, fatty acids operate as protonophores in the physiological pH range,

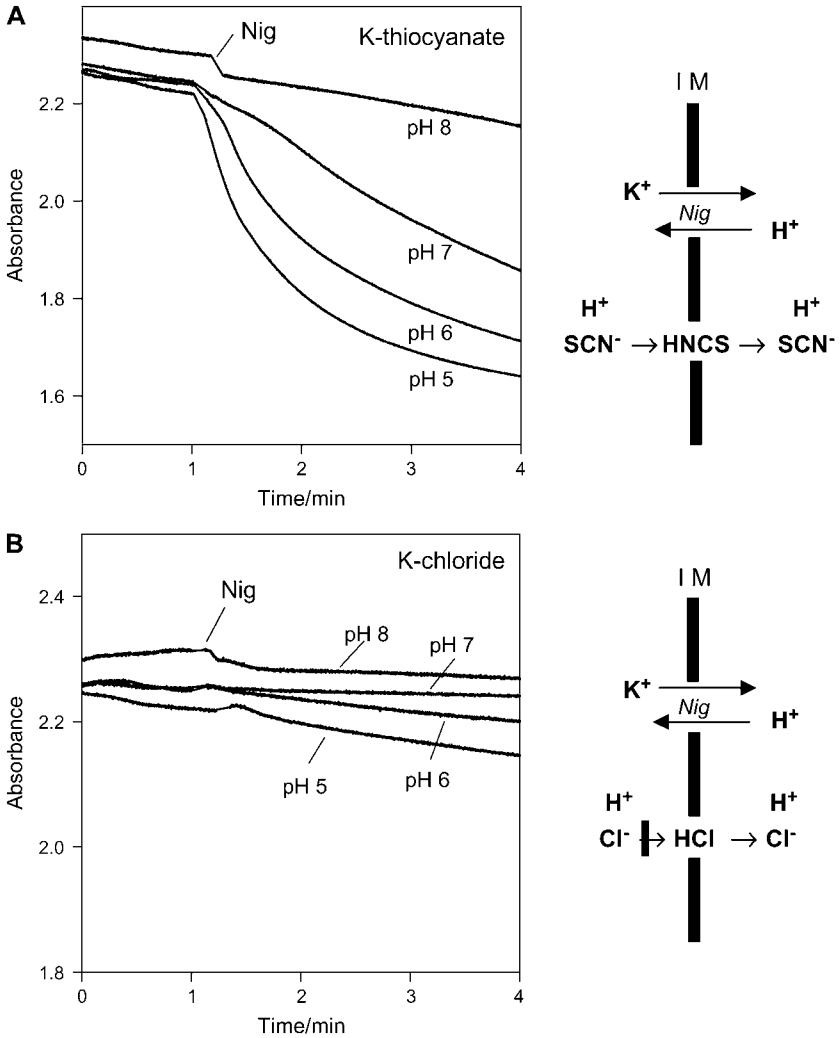

FIGURE 3 Induction of membrane permeability to potassium thiocyanate by nigericin and acidification of medium pH. Mitochondria (1 mg of protein/mL) were suspended in K-thiocyanate or K-chloride medium adjusted to pH values as indicated. Nigericin was added as in Fig. 2.

despite a relatively low pKa (4.9) of the carboxyl group (39). However, it is also known that the incorporation of fatty acids into membranes shifts their pKa in the physiological range (40). In analogy, there is reason to assume that the proton affinity of SCN^- anion increases at the medium/interface due to a changed environment. In addition, mitochondria were exposed to a high concentration of SCN^-, so that even a very small percentage of thiocyanate protonation is sufficient for mediating a measurable H^+ transfer. Finally, a potential protonophoric action of thiocyanate does not question its use as probe of membrane potential estimation, since membrane potentials are measured usually around pH 7 and, in addition, with a low concentration of [^{14}C]thiocyanate (41).

Test calculations on the sulfur-containing parent solute molecules

The chemical name thiocyanic acid is used in the literature although the existence of the acid has not been established so far. Thiocyanic acid was early reported as a white solid that was deposited at −190°C (42), but the structure of this substance is unknown. The formation of thiocyanic acid was only verified under matrix isolation conditions in photochemical experiments (43). On the other hand, studies by microwave spectroscopy (44), photoelectron spectroscopy/mass spectrometry (45), and ultraviolet spectroscopy (46) in the vapor phase and by infrared spectroscopy (47, 48) both in the vapor phase and by matrix isolation are rather in line with the isothiocyanic acid structure HNCS. As far as theory is concerned, calculation of ΔG^{Isom} with DFT using the basis sets 6-311++G(d,p) and 6-311++G(3df,3pd) predicts HNCS to be more stable than HSCN by 11.8 and 11.2 kcal/mol, respectively. In principle, this conclusion holds at a demanding ab initio quantum chemistry level. Even if the calculation by Gaussian-3 theory predicts lower energies of isomerization ($\Delta G^{Isom} = 8.6$ kcal/mol), the isothiocyanic acid remains to be clearly favored over the thiocyanic acid in the gas phase. The situation in aqueous solution is less clear, for the site of protonation at the thiocyanate anion SCN^- is not experimentally known. According to DFT calculations mentioned below, the solvent water favors the isothiocyanic acid furthermore. For that reason, the term thiocyanic acid was avoided in this study.

It should only be mentioned that experimental geometries of the known sulfur-containing solute molecules are excellently reproduced theoretically. According to B3-LYP/6-311++G(d,p) calculations isothiocyanic acid, HNCS, is slightly bent. The angle of ~174.1° is in close agreement with the angle found experimentally in a combined microwave spectroscopy/near infrared spectroscopy gas phase study (174.4°) (49). The average absolute deviation between the nonhydrogen atoms amounts to only 0.001 Å. The Gibbs free energy of protonation (ΔG^{Prot}) of SCN^-, calculated as free molecules at 298.15 K, amounts to −323.8 kcal/mol with the 6-311+G(d,p) and to −325.6 kcal/mol with the 6-311++G(3df,3pd) basis set, respectively. According to the literature the experimental ΔG^{Prot} values of SCN^- are −317.4 (50) and −328.8 kcal/mol (51). For comparison, the correspondingly calculated ΔG^{Prot} values of Cl^- are −333.5 and −334.2 kcal/mol, respectively, to compare with −328.2 (52) and −327.9 kcal/mol (53) found experimentally. In absence of water the protonation energies of SCN^- and Cl^-, and correspondingly the deprotonation energies of HNCS and HCl, differ little. Thus the deprotonation in the gas phase differs greatly from that in aqueous solution. Whereas the structure of the acid is not experimentally supported in solutions, the anion SCN^- is well defined. The calculated charges at the nitrogen and sulfur atoms of the anion suggest a stronger proton affinity at nitrogen than at sulfur. The formula SCN^- was therefore preferred in this study. However, as well known, the anion's behavior is ambident (54).

The microscopic hydration model

The hydrate gas phase cluster structures calculated by DFT without consideration of the effect of bulk water are depicted in Figs. 4 and 5. The calculated hydration energies are listed in Table 1. The monohydrate of SCN^- (1a) contains a single water molecule bound to a nitrogen atom (''N-hydrate''). The gain of energy relative to the free components amounts to −14.6 kcal/mol. As indicated by one imaginary frequency, the S-monohydrate is only a transition structure. Attempts failed to find the minimum structure of this isomer. The optimization always ended in the more stable N-hydrate. Hydration at sulfur is observed with the N,S-dihydrate structure 1b. However, the N,N-dihydrate 1c is more stable than 1b by ~2 kcal/mol, and the cluster hydration energy was calculated to −26.7 kcal/mol. The H-bond between the two water ligand molecules of 1c contributes to the cluster hydration energy by ~1 kcal/mol. The N,N,S-hydrate 1d contains two water molecules at nitrogen and one at sulfur. The structure appears structurally related to the dihydrates 1b and 1c. The experimental derived intermolecular distance between SCN^- and the ligands of 2.16 Å found in the study of Kameda et al. (15) may be compared with the calculated average N···H distance of 2.08 Å. The calculated N···O distances are between 2.8 and 3.1 Å. The cluster hydration energy of 1d amounts to −35.8 kcal/mol. The addition of a fourth water molecule resulting in 1e lowered the cluster hydration energy to −47.7 kcal/mol (Table 1). As depicted in Fig. 4, one of the water molecules appears less strongly bound to SCN^-. Again, this molecule exhibits H-bonds to the adjacent water molecule. Nevertheless, O···S distances of 3.55 and 3.82 Å and O···N distances of 2.86 and 2.89 Å of 1e justify the four water molecules to attribute to the first hydration shell of SCN^-. Whereas the calculation predicts the hydration number 4 in the gas phase, the experimental

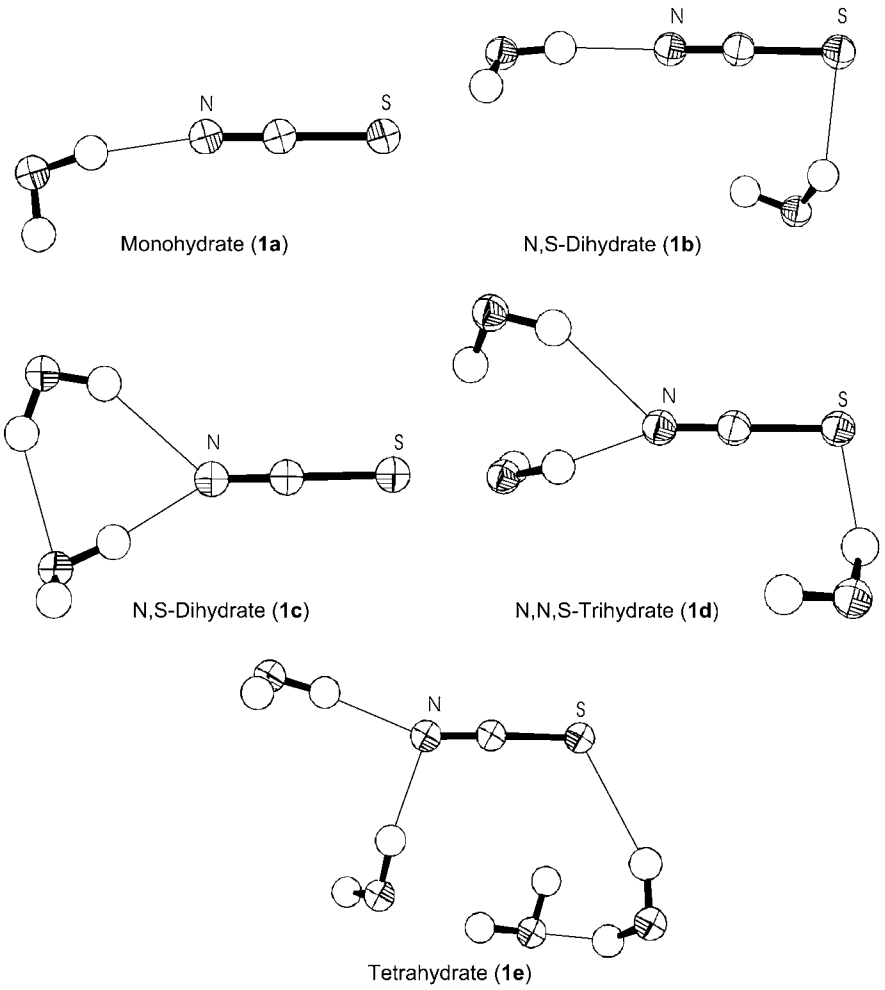

FIGURE 4 Hydrate structures of thiocyanate calculated by DFT. Thin lines indicate H-bonds between thiocyanate and water or between water molecules.

value is lower with ~2 water molecules found under thermal conditions in the liquid (15).

In contrast to SCN^-, the chloride anion is inclined to higher coordination of water and larger binding energies. The calculated structures are depicted in Fig. 5, and the energies are assembled in Table 1. The monohydrate 2a displays the intermolecular $O^{\cdots}Cl$ distance at 3.14 Å, and the distances mostly increase when going from lower to higher hydration numbers (up to 3.35 Å with $N = 5$). In contrast to the dehydrate 2c the two water ligands of 2b take the opposite position. Similarly, there are two isomeric trihydrates, 2d and 2e. In the case of higher hydration numbers, the ligands are in close vicinity. The trihydrates 2d and 2e and the tetrahydrate 2f were already derived by MP2 calculations (26). Using DFT we succeeded in getting the pentahydrate 2g of the same type of structure. This hydrate displays C_s symmetry and is stabilized by −65.1 kcal/mol. With five ligand molecules the first hydration shell of Cl^- is obviously complete. There are three different $O^{\cdots}Cl$ distances of 3.00 (1x), 3.34 (2x), and 3.47 Å (2x), respectively. As mention before, there is a competition between ion-water H-bonds and the H-bonds between water molecules. The water molecules display characteristic interligand H-bonds of 2.09 and 2.14 Å. Nearly 6 kcal/mol of the cluster hydration energy of 2g is due to H-bonds between water molecules. In the hydrates of the coordination number $N = 6$ (2h), two water molecules are placed more outside by 1 Å than the remaining four water molecules. These two water molecules may be considered as part of a second hydration shell (26). The cluster hydration energy of the hexahydrate increased to −82.3 kcal/mol (Table 1).

Thus the study of the hydration of the Cl^- has shown that the first hydration shell of SCN^- contains at best four water molecules and the shell of Cl^- five molecules at best. Attempts failed to seize more water molecules close to the solute molecules within the nearest shell. With regard to the statistical distribution of the different hydrates at room temperature, the effective hydration numbers are lower.

The cluster hydration energies listed in Table 1 show clearly that SCN^- is less stabilized by hydration than Cl^-. This is shown by ΔE^{Clust} values at 0 K and the thermodynamic quantities ΔH^{Clust} and ΔG^{Clust} calculated at 298.15 K. Whereas the first column contains results from B3-LYP/6-31++G(d,p) calculations with optimum geometries,

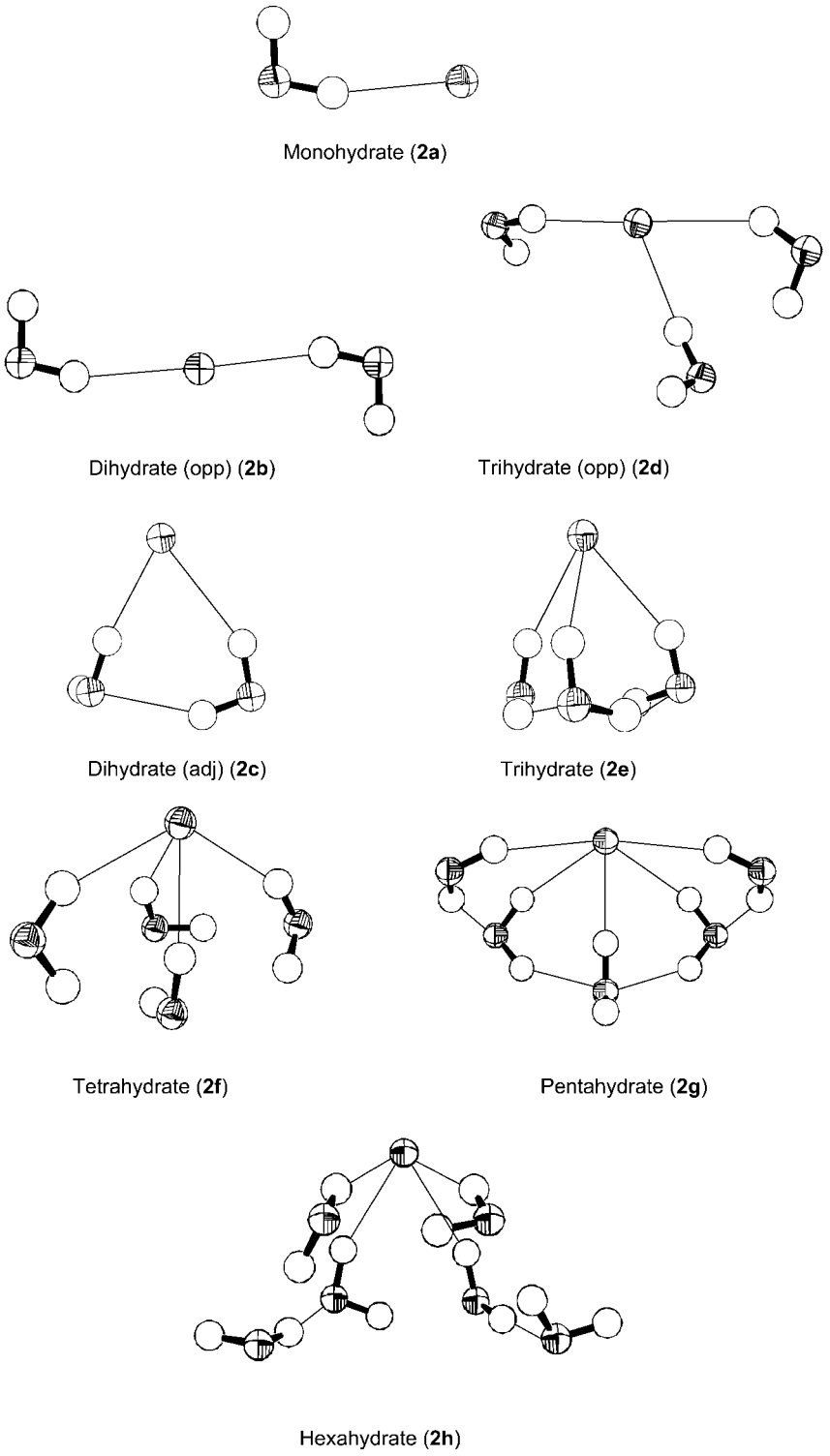

FIGURE 5 Hydrate structures of chloride calculated by DFT. Thin lines indicate H-bonds between chloride and water or between water molecules.

energies in parentheses were obtained with a more extended basis set. The extended basis set reduces basis set and BSSEs. However, the change of the numerical data is low and former conclusions are not affected. The thermodynamic quantities reflect the same order and relationships between the energies values as calculated at 0 K (Table 1). The low Gibbs free energies ΔG^{Clust} relative to the enthalpies ΔH^{Clust} of hydration are due to the fact that hydration is disfavored by entropy. In terms of free energy, the stabilization of SCN^- by the solvent is again half as large as Cl^-.

The acids HNCS and HCl are less solvated than the related anions. The hydration free energies of the acids, not listed in

TABLE 1 Cluster hydration energies ΔE^{Clust}, Gibbs free energies ΔG^{Bind}, and enthalpies ΔH^{Bind} of hydrated SCN^- and Cl^- calculated by DFT

		Calculation			Experiment
	Shell*	$\Delta E^{Clust\dagger}$	$\Delta G^{Clust\ddagger}$	$\Delta H^{Clust\ddagger}$	$\Delta^{Exp\S}$
1a	$N = 1$ (N)	−14.6 (−13.7)	−5.4	−12.9	–
1b	$N = 2$ (NS)	−24.7 (−23.6)	−7.8	−21.4	–
1c	$N = 2$ (NN)	−26.7 (−25.1)	−6.9	−23.2	–
1d	$N = 3$ (NNS)	−35.8 (−32.7)	−6.2	−31.5	–
1e	$N = 4$	−47.7 (−43.6)	−7.7	−40.6	–
2a	$N = 1$	−14.9 (−14.7)	−8.4	−14.5	−14.7
2b	$N = 2$ (opp)	−27.9 (−27.1)	−15.0	−26.2	
2c	$N = 2$ (adj)	−28.0 (−27.2)	−12.3	−27.2	−27.7
2d	$N = 3$ (opp)	−41.3 (−40.0)	−16.8	−37.8	
2e	$N = 3$ (adj)	−44.2 (−42.9)	−14.1	−39.7	−39.5
2f	$N = 4$	−55.5 (−53.4)	−15.3	−49.0	−50.1
2g	$N = 5$	−65.1 (−61.3)	−18.5	−58.3	−59.6
2h	$N = 6$	−82.3 (−75.8)	−21.8	−72.2	−68.4

N denotes the hydration number.

*The two water molecules may be situated adjacent (adj) or opposite (opp).

†The DTT cluster hydration energies were calculated using B3-LYP/6-311++G(d,p) and 6-311++G(3df,2p) based on B3-LYP/6-311++G(d,p) geometries (in parentheses).

‡Thermodynamic energies were calculated with routines of Gaussian98 for standard ambient temperature and pressure conditions.

§Experimental enthalpies were derived from consecutive dissociation energies measured by high pressure mass spectrometry (55). Energy data are given as kcal/mol.

Table 1, are ~7 kcal/mol in the case of the monohydrates and ~16 kcal/mol in the case of dihydrates. As to be expected, the most stable monohydrates are formed by H-bonds between the proton of the acids and the oxygen of water.

The excellent performance of DFT in calculating the microscopic solvation energies is shown by comparing the calculated cluster hydration enthalpies with experimental values in Table 1. The experimental enthalpies were measured by gas phase clustering reactions of Cl^- and water by means of mass spectrometry at temperatures in which the sample vapor starts to condense (55), i.e., under nearly liquid phase conditions. The average absolute error between calculated and experimental values amounts to only 1 kcal/mol.

The statistically described hydration at ambient temperature

At ambient temperature, the anion-water complex is not rigid and the individual water ligands are being continuously replaced in the nanosecond timescale. For a definite hydration number, more than one minimum structure must exist. The various complexes of a definite hydration number, N, differ, consequently, in their energies. The participation of the various structures in the effective hydration process is determined by statistics. To cope with the situation, one of us (L.M. and co-workers) developed a suitable approach (56,57). It is essentially stochastic in nature. Water molecules are randomly placed around the solute molecule, and the solvent molecules are also allowed to randomly rotate around the three coordinate axes. Along these lines a large number of solute-water aggregates may be generated. The individual structures are then optimized in energy. Along this way global as well as numerous local minima are found on the potential hypersurface. Therefore the approach was called the multiple minima hypersurface (MMH) method. Calculations were performed for different hydration numbers of the anion varying from 1 to 6, including those exceeding the nearest hydration sphere. The large demand of computer time is avoided by performing MMH calculations with a semiempirical potential (PM3 method by Stewart (58)).

Results of the structural calculation are exemplified with hexa-hydrated thiocyanates in Fig. 6. To show main features of calculated hydrate cluster structures, the four lowest-energy hydrates are taken from 100 previously optimized structures and geometrical parameters and the populations are given in Fig. 6. The population depends on the energies of the hydrates and is essentially defined by the Boltzmann weighting factors. In the calculated hydrate structures, not all of the water molecules are placed closely to thiocyanate in the nearest hydration sphere. Whereas low coordinated hydrates of SCN^- exhibit $O^{\cdots}S$ and $O^{\cdots}N$ interatomic distances between 3.4 and 3.8 Å and 2.8 and 3.1 Å, respectively, some distances of the hexa-coordinated SCN^- of Fig. 6 are considerably larger with 4.3 to 5.3 Å for $O^{\cdots}S$ and 4.4 to 6.6 Å for $N^{\cdots}O$. In the case of the structure depicted in *B* of Fig. 6, for example, the hydrate displays the expected relatively short interatomic distances between S1 and both O5 and O6 and between N1 and O4, whereas the remaining distances between the terminal hetero atoms of SCN^- and O are outside the range of the first shell. Two water molecules are obviously weakly bound through ''hydration bonds''. These water molecules are obviously part of a second or a higher solvation shell.

Within the MMH approach, the stabilization energy of the solute in the water cluster is defined as association energy (56). The reference state is the noninteracting system of the solute and solvent molecules. Because of the statistical definition of the energy over a series of structures rather than only a single structure and the different theoretical model used, MMH association energies are not comparable with the DFT cluster hydration energies as described above.

Gibbs free energies of association (ΔG^{Assoc}) were calculated for Cl^- and SCN^- with the hydration numbers $N = 1$ to $N = 6$. Remarkably, these association energies led to the same prediction about the relative strength of the hydration of the anion as found by cluster hydration energies 0 K. The energies of SCN^- are for all hydration numbers significantly weaker than for Cl^-. To give an example, ΔG^{Assoc} of the hydrates of SCN^- with the hydration number $N = 5$ was calculated to −34.5 kcal/mol. In contrast, the energy is about twice as large for the hydrates of Cl^-, calculated to −63.0 kcal/mol with the same hydration number. The entropic term ΔS^{Assoc} does not affect this conclusion.

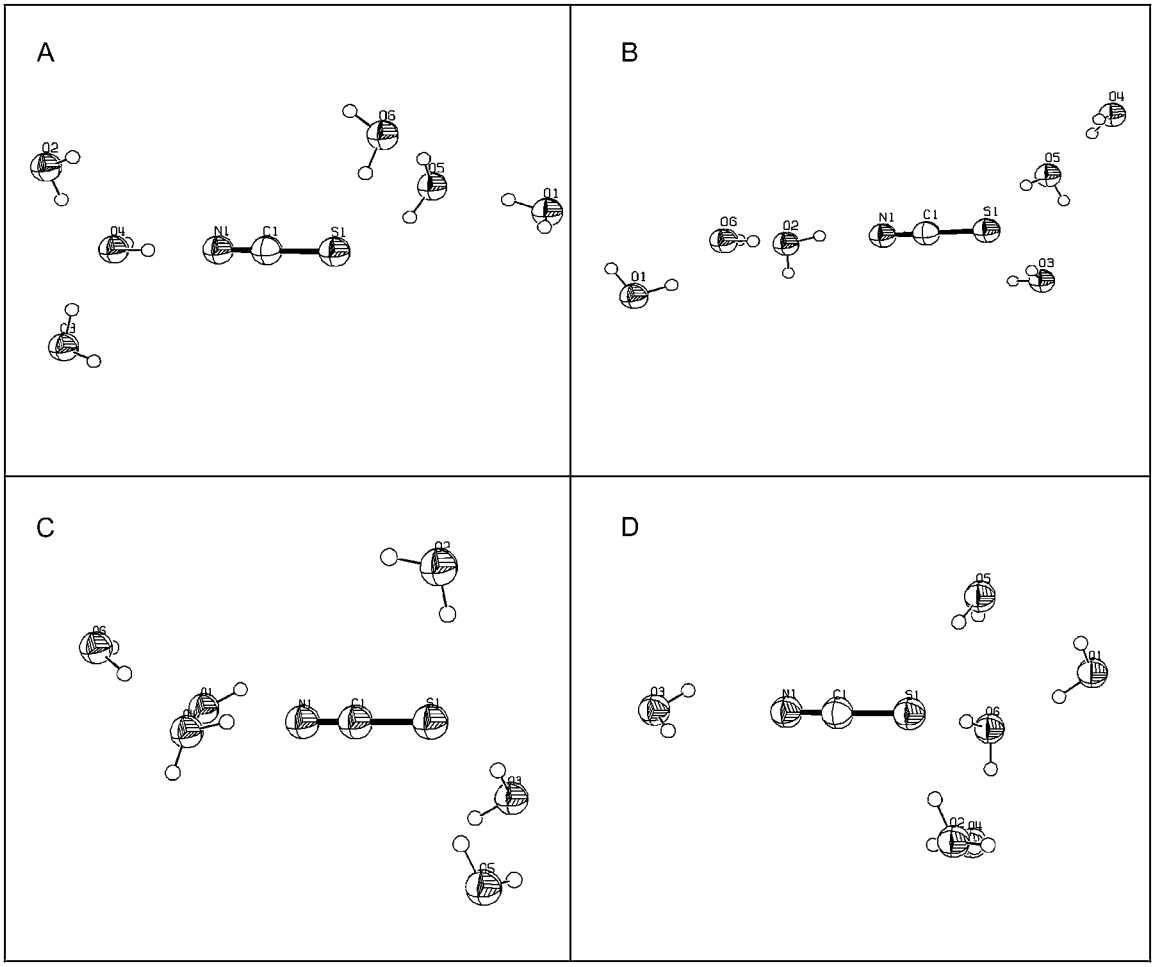

FIGURE 6 Four lowest energy structures obtained after optimization starting from a series of 100 SCN^- hexahydrate random molecular arrangements. (*A*) The structure of *A* contributes to 2.5% of the total population. Two water molecules constitute the inner shell of hydration at S and only one at N. The remaining water molecules result in ''hydrating water''. (*B*) The structure of *B* contributes to 2.0% of the total population. Two water molecules constitute the inner shell of hydration at S and only one at N. The remaining water molecules result in ''hydrating water''. (*C*) The structure *C* contributes to 1.9% of the total population. Three water molecules constitute the inner shell of hydration at S and only one at N. The remaining water molecules result in ''hydrating water''. (*D*) The structure of *D* contributes to 1.9% of the total population. Three water molecules constitute the inner shell of hydration at S and only one at N. The remaining water molecules result in ''hydrating water''.

Hydration with consideration of the dielectric continuum

The solute molecules are inscribed in a cavity surrounded by the water continuum and were calculated by PCM-DFT. The gain in free energy of the solute in the dielectric continuum is denoted with ΔG^{Cont}. The calculated energies are collected in Table 2. The solvation energies are small for the acids HCl and HSCN and large for the bare ions Cl^- and SCN^-. If microhydration is disregarded, the free energy of solvation of Cl^- is calculated to $\Delta G^{\mathrm{Cont}} = -76$ kcal/mol. As already found by Tomasi et al. (32), the PCM solvation energy of the chloride is close to the experimental total hydration energy. Calculated under the same conditions, SCN^- is however stabilized by only -57.7 kcal/mol in water and thus much less than Cl^-. The PCM solvation energies of the hydrated Cl^- and SCN^- are lower than those of the bare ions. The solvation energies considerably decrease with the hydration number (Table 2).

Based on the hybrid supermolecule-continuum model, approximate hydration energies ΔG^{Hydr} of SCN^- and Cl^- were estimated by adding the calculated free energies of the water-anion cluster $\Delta G^{\mathrm{Clust}}$ calculated in the gas phase and the free energies ΔG^{Cont} of the pure dielectric continuum approach calculated in solution. As found for ΔG^{Cont}, the energy ΔG^{Hydr} decreases with the hydration number. With the experimental hydration number $N = 2$ of SCN^- (15) the total hydration energy amounts to 57.2 kcal/mol, whereas the energy of Cl^- is 72.1 kcal/mol (exp. hydration energies values are between 71 and 83 kcal/mol, see Topol et al. (23)). Fig. 7 shows the total hydration energies as resulting from the cluster hydration energies with -12.3 kcal/mol for

TABLE 2 Free energies ΔG^{Cont} of hydrate clusters in the dielectric continuum calculated by PCM-DFT* and total free energies $\Delta G^{Hydr\dagger}$ of hydration in kcal/mol

	Shell	ΔG^{Cont}	ΔG^{Hydr}		Shell	ΔG^{Cont}	ΔG^{Hydr}
SCN^-	$N = 0$	−57.7	–	Cl^-	$N = 0$	−76.0	–
$HNCS^{\ddagger}$	$N = 0$	−5.4	–	HCl	$N = 0$	−0.5	–
$HNCS^{\ddagger}$	$N = 2$	−3.1	−7.7	HCl	$N = 2$	−5.3	−9.8
1a	$N = 1$ (N)	−52.3	−57.7	2a	$N = 1$	−68.0	−76.4
1b	$N = 2$ (NS)	−46.8	−57.2	2c	$N = 2$	−59.8	−72.1
1c	$N = 2$ (NN)	−49.4	−53.7	2e	$N = 3$	−50.0	−64.1
1d	$N = 3$ (NNS)	−45.8	−52.0	2f	$N = 4$	−43.9	−59.1
1e	$N = 4$	−42.5	−50.2	2g	$N = 5$	−41.0	−59.5
				2h	$N = 6$	−39.6	−61.4

N denotes the hydration number.

*PCM-DFT single point calculations with B3-LYP/6-311++G(d,p).

†Approximate ΔG^{Hydr} energies calculated from ΔG^{Clust} of the gas phase hydrate clusters (Table 1) and ΔG^{Cont} obtained of the dielectric continuum approach.

‡Solvation energy ΔG^{Cont} of HSCN ($N = 0$) amounts to −3.7 kcal/mol compared with −5.4 kcal/mol calculated for HNCS. This means HNCS experiences additional stabilization relative to HSCN in passing from gas phase to the aqueous solution. The isomerization energy ΔG^{Isom} increases from 11.8 without solvent effect to 13.5 kcal/mol in solution.

chloride dihydrate and −6.9 kcal/mol for thiocyanate dihydrate and the energies of these dihydrates in the dielectric continuum (−59.8 and −46.8 kcal/mol, respectively).

At any rate, for comparable hydration numbers the difference in the hydration free energies ΔG^{Hydr} between Cl^- and SCN^- consistently confirms a lower net stabilization of SCN^- than of Cl^- in water. The particular position of SCN^- in solvation revealed with the study of the microsolvation is retained in bulk water.

CONCLUSIONS

Mitochondria swell in K-thiocyanate medium in the presence of nigericin when the medium pH becomes acidic, unlike K-chloride medium. This finding clearly indicates that a H^+ flux takes place from the medium across the mitochondrial inner membrane to the matrix of mitochondria. A protonophoric mechanism depends on the permeation of thiocyanate and of its protonated form, isothiocyanic acid. From previous studies (3,8), it is known that hydrogen chloride and isothiocyanic acid permeate planar bilayer membranes rapidly, indicated from similar permeabilities of 2.9 cm/s and 2.6 cm/s, respectively. This fact clearly suggests that anion permeation is the rate limiting step within the protonophoric mechanism. Accepting a ''solubility-diffusion'' mechanism, one has to take into consideration two types of free energy changes of the thiocyanate-mediated proton transfer. These free energy changes are ascribed to i), the dehydration of thiocyanate near the medium-membrane interface (ΔG^{Hydr}), and ii), the formation of HNCS by protonation of nonhydrated thiocyanate (ΔG^{Prot}). Measured as well as the calculated gas phase deprotonation enthalpies of HNCS and HCl does not indicate that an essential difference in ΔG^{Prot} for HNCS and HCl is a contributing factor of the protonophoric activity.

In the discussion of hydration/dehydration processes, we have used quantum chemical methods. First we have investigated the structure of the nearest hydration shell and the number of solvent molecules that are placed in the shell. Second, we have modeled the rest of the solvent with a dielectric continuum model by using both the anion and the hydrated anions as solutes. Hydration energies were estimated by the combination of the results of the microscopic cluster calculation and the calculation of the bulk water effect within a supermolecule-continuum model at the DFT level. The conclusion based on the relative total hydration free energies is unequivocal: The energy of SCN^- is significantly less than the energy of Cl^-. The distinctly different anion stabilization is already evident in the cluster hydration energies of the anions derived for the global minima on the hypersurface at 0 K and, in more flexible arrangements, statistically on the multiple minimum hypersurface at ambient

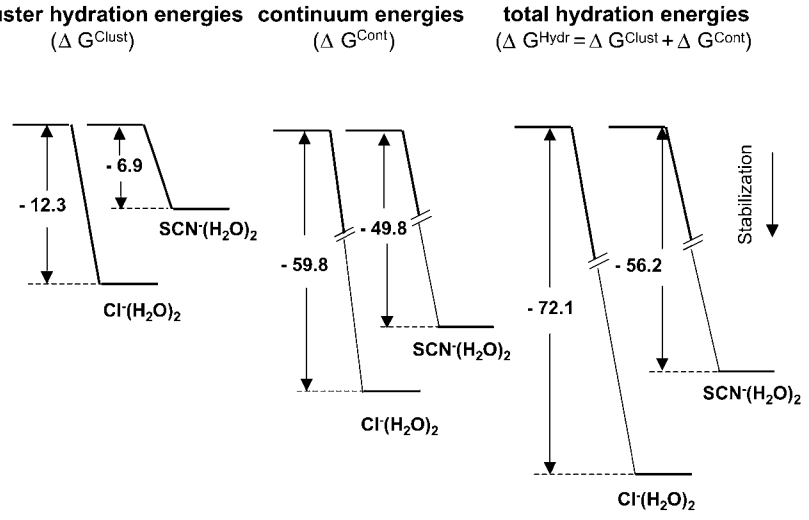

FIGURE 7 Visualization of the lower solvent stabilization of thiocyanate relative to chloride by Gibbs free hydration energies calculated by different theoretical models. Microscopic cluster hydration energies and solvent energies of the hydrates in the dielectric continuum result in total hydration energies.

temperatures. According to the DFT cluster hydration and MMH association energies, the energetic stabilization of SCN^- hydrates is about half as large as the stabilization of Cl^- hydrates. Consequently, thiocyanate is much less prone to hydration than chloride, and consequently much more easily prone to dehydration.

In view of the need to strip off the hydration shell before transmembrane permeation, the particular position of thiocyanate may be understood. In summary, the protonophoric activity of thiocyanate is governed by free energy changes of thiocyanate dehydration (ΔG^{Hydr}) and of protonation of thiocyanate (ΔG^{Prot}). A stronger hydration prevents chloride from operating as a protonophore. Finally, the results obtained in this study support the concept that the inhibition of gastric acid secretion by thiocyanate is due to its protonophoric activity.

Promising approaches for future studies in describing the transfer of ions along the biological channel offer the recently advanced empirical MD (59) and the QM/MM Car-Parinello MD methods (60).

We are indebted to Ralf Bohnensack (Otto-von-Guericke-University Magdeburg) for valuable comments on this article.

REFERENCES

1. Helander, H. F., and D. J. Keeling. 1993. Cell biology of gastric acid secretion. *Baillieres Clin. Gastroenterol.* 7:1–21.
2. Davenport, H. W. 1940. The inhibition of carbonic anhydrase and of gastric secretion by thiocyanate. *Am. J. Physiol.* 129:505–514.
3. Gutknecht, J., and A. Walter. 1982. SCN^- and HSCN transport through lipid bilayer membranes. A model for SCN^- inhibition of gastric acid secretion. *Biochim. Biophys. Acta.* 685:233–240.
4. Reenstra, W. W., and J. G. Forte. 1983. Action of thiocyanate on pH gradient formation by gastric microsomal vesicles. *Am. J. Physiol.* 244:G308–G313.
5. Reenstra, W. W., and J. G. Forte. 1986. Mechanism of inhibition of gastric acid secretion by SCN^-: interrelation of SCN^- flux and inhibition. *Am. J. Physiol.* 250:G76–G84.
6. Wolosin, J. W., and J. G. Forte. 1983. Anion exchange in oxyntic cell apical membrane: relationship to thiocyanate inhibition of acid secretion. *J. Membr. Biol.* 76:261–268.
7. Chiang, Y., and A. J. Kresge. 2000. Determination of the acidity of isothiocyanic acid aqueous solution. *Can. J. Chem. / Rev. Canad. Chim.* 78:1627–1628.
8. Gutknecht, J., and A. Walter. 1981. Transport of protons and hydrochloric acid through lipid bilayer membranes. *Biochim. Biophys. Acta.* 641:183–188.
9. Dawson, D. C., S. S. Smith, and M. K. Mansoura. 1999. CFTR: mechanism of anion conduction. *Physiol. Rev.* 79:S47–S75.
10. Dilger, J. P., S. G. McLaughlin, T. J. McIntosh, and S. A. Simon. 1979. The dielectric constant of phospholipid bilayers and the permeability of membranes to ions. *Science.* 206:1196–1198.
11. Paula, S., A. G. Volkov, and D. W. Deamer. 1998. Permeation of halide anions through phospholipid bilayers occurs by the solubility-diffusion mechanism. *Biophys. J.* 74:319–327.
12. Jorgensen, W. L. 1989. Free energy calculations: a breakthrough for modeling in organic chemistry in solution. *Acc. Chem. Res.* 22: 184–189.
13. Asthagari, D., L. R. Pratt, and H. S. Ashbaugh. 2003. Absolute hydration energies of ions, ion-water clusters, and quasichemical theory. *J. Chem. Phys.* 119:2702–2708.
14. Sansone, R., C. Ebner, and M. Probst. 2000. Quantum chemical and molecular dynamic study on the hydration of cyanide and thiocyanate anions. *J. Mol. Liq.* 66:129–150.
15. Kameda, Y., R. Takahashi, T. Usuki, and O. Uemura. 1994. Hydration structure of SCN^- in concentrated aqueous solutions. *Bull. Chem. Soc. Jpn.* 67:956–963.
16. Mason, P. E., G. W. Neilson, C. J. Dempsey, A. C. Barnes, and N. M. Cruckishank. 2003. The hydration structure of guanidinium and thiocyanate ions: implications for protein stability in aqueous solution. *Proc. Natl. Acad. Sci. USA.* 100:4557–4561.
17. Tobias, D. J., P. Jungwirth, and M. Parrinello. 2001. Surface solvation of halogen ions in water clusters: an *ab initio* molecular dynamics study of the $Cl^-(H_2O)_6$ complex. *J. Chem. Phys.* 114:7036–7044.
18. Henft, J. M., and E. J. Meijer. 2003. Density functional theory based molecular-dynamical study in aqueous chloride solvation. *J. Chem. Phys.* 119:11788–11793 (and references therein).
19. Degrève, L., V. M. de Pauli, and M. A. Duarte. 1997. Simulation study of the role and structure of monoatomic ions multiple hydration shells. *J. Phys. Chem.* 106:655–665.
20. Tongraar, A., and B. M. Rode. 2003. The hydration structures of F^- and Cl^- investigated by *ab initio* QM/MM molecular dynamics simulation. *Phys. Chem. Chem. Phys.* 5:357–362.
21. Bergström, P. A., J. Lindgren, and O. Kristiansson. 1991. An IR study of the hydration of perchlorate, nitrate, iodide, bromide, chloride and sulfate anions in aqueous solution. *J. Phys. Chem.* 95:8575–8580.
22. Tuñón, I., E. Silla, and J. Bertran. 1993. Proton solvation in liquid water. An ab initio study using the continuum model. *J. Phys. Chem.* 97:5547–5552.
23. Topol, I. A., G. J. Tawa, S. K. Burt, and A. A. Rashin. 1999. On the structure and thermodynamics of solvated monoatomic ions using a hybrid solvation model. *J. Chem. Phys.* 111:10998–11014.
24. Zhan, C.-G., and D. A. Dixon. 2004. Hydration of the fluoride anion: structures and absolute hydration free energy from first-principles electronic structure calculations. *J. Phys. Chem. A.* 108:2020–2029.
25. Nicholls, D. G., and S. J. Ferguson. 2002. Bioenergetics 3. Academic Press, Amsterdam.
26. Gora, R. W., S. Roszak, and J. Lzczynsky. 2000. Properties and nature of interaction in $Cl^-(H_2O)_n$ n=1,6 clusters: a theoretical study. *Chem. Phys. Lett.* 325:7–14.
27. Koch, W., and M. C. Holthausen. 2000. A Chemist's Guide for Density Functional Theory. Wiley-VCH, Weinheim.
28. Zhou, Z., Y. Shi, and X. Zhou. 2004. Theoretical studies on the hydrogen bonding interaction of complexes of formic acid with water. *J. Phys. Chem. A.* 108:813–822.
29. Hobza, P., J. Sponer, and T. Reschel. 1995. Density functional theory and molecular clusters. *J. Comput. Chem.* 16:1315–1325.
30. Masao, M. 2001. The effect of basis set superposition error on the convergence of interaction energies. *Theor. Chem. Acc.* 106:301–313.
31. Satchell, J. F., and B. J. Smith. 2002. Calculations of aqueous dissociation constants of 1,2,4.triazole and terazole. A comparison of solvation models. *Phys. Chem. Chem. Phys.* 4:4314–4318.
32. Tomasi, J., and B. Mennucci. 1997. Self-consistent reaction field methods. *In* Encyclopedia of Computational Chemistry, Vol. 4. P. von Ragué Schleyer, editor. J. Wiley, Chichester. 2547–2551.
33. Florián, J., and A. Warshel. 1997. Langevin dipoles model for ab initio calculations of chemical processes in solution; parametrization and applications to hydration free energies of neutral and ionic solutes and conformational analysis in aqueous solution. *J. Phys. Chem. B.* 101: 5583–5595.
34. Cammi, R., B. Beneddetta, and J. Tomasi. 2003. Computational modelling of the solvent effects on molecular properties: an overview of the polarizable continuum (PCM) approach. *Comput. Chem.* 8:1–79.

35. Tomasi, J. 2004. Thirty years of continuum solvation chemistry: a review, and prospects for the near future. *Theor. Chem. Acc.* 112: 184–203.

36. Frisch, M. J., G. W. Trucks, H. B. Schlegel, G. E. Scuseria, M. A. Robb, J. R. Cheeseman, V. G. Zakrzewski, J. A. Montgomery Jr., R. E. Stratmann, J. C. Burant, S. Dapprich, J. M. Millam, A. D. Daniels, K. N. Kudin, M. C. Strain, O. Farkas, J. Tomasi, V. Barone, M. Cossi, R. Cammi, B. Mennucci, C. Pomelli, C. Adamo, S. Clifford, J. Ochterski, G. A. Petersson, P. Y. Ayala, Q. Cui, K. Morokuma, D. K. Malick, A. D. Rabuck, K. Raghavachari, J. B. Foresman, J. Cioslowski, J. V. Ortiz, A. G. Baboul, B. B. Stefanov, G. Liu, A. Liashenko, P. Piskorz, I. Komaromi, R. Gomperts, R. L. Martin, D. J. Fox, T. Keith, M. A. Al-Laham, C. Y. Peng, A. Nanayakkara, C. Gonzalez, M. Challacombe, P. M. W. Gill, B. Johnson, W. Chen, M. W. Wong, J. L. Andres, C. Gonzalez, M. Head-Gordon, E. S. Replogle, and J. A. Pople. 1998. GAUSSIAN 98, Revision A.7. Gaussian, Inc., Pittsburgh, PA.

37. Barone, V., M. Cossi, and J. Tomasi. 1997. A new definition of the cavity for the computation of free energies by the polarizable continuum model. *J. Chem. Phys.* 107:3210–3221.

38. Beavis, A. D. 1992. Properties of the inner membrane anion channel in intact mitochondria. *J. Bioenerg. Biomembr.* 24:77–90.

39. Wojtczak, L., and P. Schönfeld. 1993. Effect of fatty acids on energy coupling processes in mitochondria. *Biochim. Biophys. Acta.* 1183:41–57.

40. von Tscharner, V., and G. K. Radda. 1981. The effect of fatty acids on the surface potential of phospholipid vesicles measured by condensed phase radioluminescence. *Biochim. Biophys. Acta.* 643:435–448.

41. Hoek, J. B., D. G. Nicholls, and J. R. Williamson. 1980. Determination of the mitochondrial protonmotive force in isolated hepatocytes. *J. Biol. Chem.* 255:1458–1464.

42. Birckenbach, L. 1942. Solid and liquid HSCN in relation to the H halides. *Forsch. Fortschr.* 18:232–233.

43. Wierzejewska, M., and Z. Mielke. 2001. Photolysis of isothiocyanate acid HNCS in low-temperature matrices. Infrared detection of HSCN and HSNC Isomers. *Chem. Phys. Lett.* 349:227–234.

44. Yamada, K., M. Winnewisser, G. Winnewisser, L. B. Szalanski, and M. C. L. Gerry. 1980. Ground state spectroscopic constants of $H^{15}NCS$,$HN^{13}CS$ and $HNC^{34}S$, and their molecular structure of isothiocyanic acid. *J. Mol. Spectrosc.* 79:295–313 (and references therein).

45. Ruscic, B., and J. Berkowitz. 1994. The H-NCS bond energy, ΔH_f (HNCS), ΔH_f (NCS), and IP(NCS) from photoionization mass spectrometric studies of HNCS, NCS, and $(NCS)_2$. *J. Chem. Phys.* 101: 7975–7989.

46. McDonald, J. R., V. M. Scherr, and S. P. McGlynn. 1969. Lower-energy electronic states of HNCS, NCS^-, and thiocyanate salts. *J. Chem. Phys.* 51:1723–1731.

47. Wierzejewska, M., and R. Wieczorek. 2003. Infrared matrix isolation and ab initio studies on isothiocyanic acid HNCS and its complexes with nitrogen and xenon. *Chem. Phys. Lett.* 287:169–181.

48. Durig, J. R., and D. W. Wertz. 1967. Infrared spectra of HNCS and DNCS. *J. Chem. Phys.* 46:3069–3077.

49. Ross, S. C., M. Niedenhoff, and K. M. T. Yamada. 1994. Semirigid bender determination of the quasilinear bending potential energy function of HNCS from the ground state rotational spectra. *J. Mol. Spectrosc.* 164:432–444.

50. Bradforth, S. E., E. H. Kim, D. W. Arnold, and D. M. Neumark. 1993. Photoelectron spectroscopy of CN^-, NCO^-, and NCS^-. *J. Chem. Phys.* 98:800–810.

51. Bierbaum, V. M., J. J. Grabowski, and C. H. DePuy. 1984. Gas-phase synthesis and reactions of nitrogen- and sulfur-containing anions. *J. Phys. Chem.* 88:1389–1393.

52. Fujio, M., R. T. McIver, and R. W. Taft. 1981. Effects of the acidities of phenols from specific substituent-solvent interactions. Inherent substituent parameters from gas-phase acidities. *J. Am. Chem. Soc.* 103: 4017–4029.

53. Trainham, R., G. D. Fletcher, and D. J. Larson. 1987. One- and two-photon detachment of the negative chlorine ion. *J. Phys. B At. Mol. Opt. Phys.* 20:L777–L784.

54. Loos, R., S. Kobayashim, and H. Mayr. 2003. Reactivity of the thiocyanate anion revisited. Can the product ratio be explained by the hard soft acid base principle? *J. Am. Chem. Soc.* 125:14126–14132.

55. Hiraoka, K., and S. Mizuse. 1987. Gas-phase solvation of Cl^- with H_2O, CH_3OH, C_2H_5OH, *i*-C_3H_7OH, *n*-C_3H_7OH and *t*-C_4H_9OH. *Chem. Phys.* 118:457–466.

56. Montero, L. A., A. M. Esteva, J. Molina, A. Zapardiel, L. Hernandez, H. Marquez, and A. Acosta. 1998. Approach to analytical properties of 2,4-diamino-5-phenyl-thiazole in water solution. Tautomerism and dependence on pH. *J. Am. Chem. Soc.* 120:12023–12033.

57. Montero, L. A., J. Molina, and J. Fabian. 2000. Multiple minima hypersurface of water clusters for calculations of association energy. *Int. J. Quantum Chem.* 79:8–16.

58. Stewart, J. J. P. 1989. Optimization of parameters for semiempirical methods. *J. Comput. Chem.* 10:209– 220,221–264.

59. Burykin, A., and A. Warshel. 2003. What really prevents proton transport through Aquaporin? Charge self-energy versus wire proposals. *Biophys. J.* 85:3696–3706.

60. Bucher, D., U. Rothlisberger, L. Guidoni, and C. Paola. 2004. QM/MM Car-Parinello molecular dynamics of the selectivity in a potassium channel. *Abstract of Papers*, *228th ACS National Meeting*. Philadelphia, PA.